



Impact of stellar variability on the observational appearance of protoplanetary disks

MASTER THESIS

in fulfillment of the requirements for the Degree of

Master of Science

in Computational Science and Engineering with Physics
submitted to the Faculty of Computer Science and Electrical Engineering,
University of Rostock

Author: Alexandra Botnariuc

Advisor: Prof. Dr. S. Wolf, CAU Kiel

Co-advisor: Prof. Dr. R. Redmer, Universität Rostock

Rostock, 11 February 2019

Abstract

Summary here!

Contents

| | | |
|----------|--|-----------|
| 1 | Introduction | 1 |
| 2 | Theory | 5 |
| 2.1 | Star Formation | 5 |
| 2.1.1 | Star forming regions | 5 |
| 2.1.2 | Star formation phases | 7 |
| 2.2 | Radiation | 8 |
| 2.2.1 | Absorption, emission and scattering | 9 |
| 2.2.2 | Blackbody radiation | 11 |
| 2.2.3 | Radiative Transfer | 13 |
| 2.3 | Stellar properties | 16 |
| 2.3.1 | Effective Temperature T_e [K] | 16 |
| 2.3.2 | Luminosity L_\star [L_\odot] | 17 |
| 2.3.3 | Stellar Mass M_\star [M_\odot] | 18 |
| 2.3.4 | Spectra | 19 |
| 2.3.5 | HR Diagram | 21 |
| 2.3.6 | Variable Stars | 22 |
| 2.3.7 | T Tauri stars | 25 |
| 2.4 | Circumstellar Disks | 25 |
| 2.4.1 | Interstellar Dust | 28 |
| 3 | Method | 31 |
| 3.1 | T Tauri Data | 31 |
| | Bibliography | 37 |

Chapter 1

Introduction

“The imagination of nature is far, far greater than the imagination of man”

— Richard Feynman, *The Values of Science*, 1955

The Universe contains the entirety of space, time, matter, and energy. Its vastness lies beyond human comprehension. Though the universe may be boundless and infinite, it is impossible at any given point in the universe to observe regions which lie further than the path light can travel in an interval of time equal to the age of the universe (13.79 billion years [10]). Therefore the sphere with an approximately 10^{26} meter radius, centered at Earth, is known as the *Observable Universe* [9] – beyond its boundaries no type of radiation can be observed.

In the generally accepted Big Bang Theory (Figure 1.1), the early Universe could be described as an intensely hot plasma, in which particles could not form atoms. As space expanded, and the temperatures dropped, in approximately 300 000 years after the "birth" of the Universe, mostly hydrogen (76%) and helium (24%) atoms with traces of lithium and deuterium formed. The remnant of the radiation emitted as the Universe became transparent at about 3000 K is commonly called the Cosmic Microwave Background or CMB – it shows the wavelength dependence of a "blackbody" radiator at about 2.7 Kelvin [5]. In the next period, known as the Dark Ages, the Universe was filled with gas atoms, but there was no starlight. Over the course of hundreds of millions of years (100 - 300 Myr), the Universe continued to expand and cool, until gravity drove matter to collapse into clusters, stars and galaxies. This is the beginning of the current era of the Universe, called the Stellar Epoch.

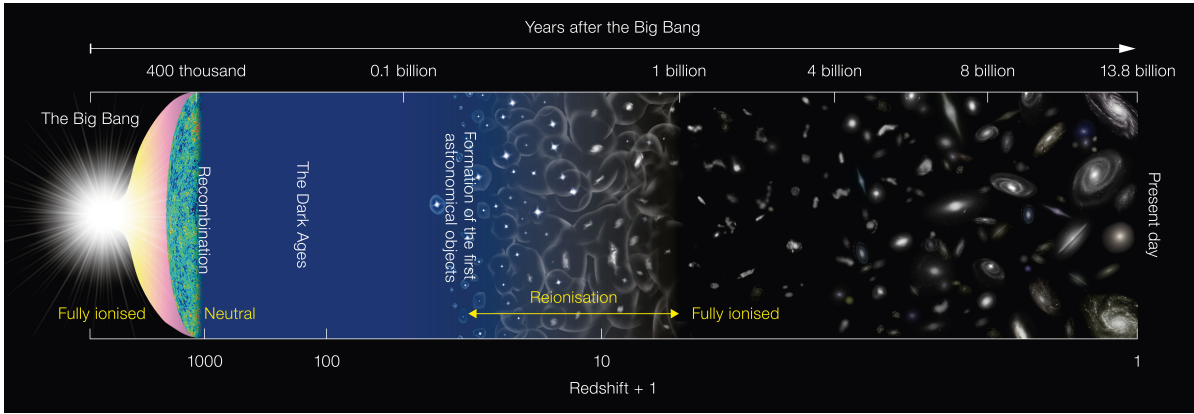


Figure 1.1: Depiction of the evolution of the Universe according to the Big Bang theory over approximately 13.8 billion years, from the beginning to the present. This image is not to scale. **Credit:** ESO/NAOJ (<https://www.eso.org/public/images/eso1620a/>)

The first stars that formed, were made of hydrogen and helium and were probably very large and very hot, possibly ending in hypernovae or even black holes. During their existence the stars have fused new elements: carbon, oxygen, silicon and iron. During their violent deaths heavier elements such as barium or lead were formed. The process of cosmic enrichment with new elements continued with the subsequent star generations. Nevertheless, the abundance of elements other than hydrogen and helium is less than 2%.

The low incidence of the elements essential for life is quite astonishing, even if the only life form known to man so far is the one on Earth. Given the size and variety in the Universe, the possibilities that other civilizations exist should be greater than null. One can calculate, using *Drake's Equation* below, the number of civilisations N in our Galaxy with whom it would potentially be possible to communicate:

$$N = R_* \cdot f_p \cdot n_e \cdot f_l \cdot f_i \cdot f_c \cdot L. \quad (1.1)$$

Equation (1.1) follows a straight forward train of thought. One should consider the rate of formation of new stars R_* in the Milky Way, which is approximately 50 new stars per year (50yr^{-1}). Out of these stars almost 50% ($f_p \approx 0.5$) will form planets. Out of the planets 40% ($n_e = 0.4$) would be inhabitable, and 90% ($f_l = 0.9$) will actually develop life. It is possible that 10% ($f_i = 0.1$) of the life forms develop into intelli-

gent life forms, and only a furthur fraction of 10%($f_c = 0.1$) will be able to achieve interstellar communication. One such civilization is estimated to have a lifetime of $L = 10000$ years. Puting all the numbers into the original equation (1.1), we obtain an estimated 900 such civilizations in our Galaxy alone. The longer these civilizations are considered to be able to exist, the higher the number of possible civilizations. The uncertainty in the factors grows for each term from left to righ, with the star formation rate being the most accurate.

It is therefore, if not interesting, at least important to study young solar systems with planet forming conditions in order to better understand nature and the origin of life. The first challenge is the size of the Universe, especially in the context of obser-vations, and the investigation of this thesis is limited to a tiny piece of the universal puzzle, that of the influence of the variability of the central star on the observation of planet forming regions surrounding stars.

Chapter 2

Theory

2.1 Star Formation

2.1.1 Star forming regions

A great part of the matter in the universe exists in the form of rarefied (low-density) gas in galaxies and around them. The gas is mostly composed of hydrogen and helium atoms, mixed with other chemical elements and dust. Inside the galaxies the gas and dust form the *Interstellar Medium* or ISM. In terms of the baryonic mass, 99% of the ISM is made up of hydrogen and helium gas, while the rest of 1% is interstellar dust and other elements. The dust is mostly solid granules (0.01 to 0.1 μm) made out of carbon, silicates (silicon and oxygen compounds) or iron and can be covered with ice. The denser areas in the ISM are called interstellar clouds, nebulae or molecular clouds, which vary in size and composition type (Figure 2.1).

It is clear from both observations and theory that star formation takes place in the coolest and densest regions of the interstellar gas: molecular clouds are practically the site of all star formation in the Galaxy. The clouds show structure on a wide variety of length scales and are somewhat arbitrarily subdivided into clumps, with characteristic masses of $10^3 - 10^4 \text{ M}_\odot$, radii $2 - 5 \text{ pc}^1$, temperature 10 K, mean number density of H_2 of $10^2 - 10^3 \text{ cm}^{-3}$. Random velocities, estimated at 2 – 3 km/s, are observed in the clumps, calculated from the width (at half-maximum intensity) of Doppler-broadened molecular lines ². The motion is caused by a combination of the thermal particle mo-

¹pc = parsec, a unit of distance see Appendix

²More about this in section 2.2.1

tion and larger-scale gas motion, probably turbulent motions and/or magnetic Alfvén waves. Embedded in the clumps are the higher-density cloud cores, whose masses can range from 1 to $1000 M_{\odot}$, with sizes of $0.05 - 0.1$ pc, temperature 10 K, mean number density of H_2 of $10^4 - 10^5 \text{ cm}^{-3}$ [3].



(a) Messier 78 Nebula ¹



(b) Barnard 59, part of the Pipe Nebula ²

Figure 2.1: The dark areas in the figures above are highly dense accumulation of gas, which absorb most of the visible light from the stars behind them. Inside them are so called "star-nurseries" or star forming regions. The blue regions visible in 2.1a are caused by reflection of starlight by a high concentration of interstellar dust. The red regions, also visible in 2.1a, are caused by emission of the heated ISM.

An overall, definitive theoretical calculation of star formation is not yet available, given that, apart from complex calculation, the initial conditions are unknown. Qualitatively, it is clear that even the relatively small-scale molecular cloud cores have far too much angular momentum to be able to collapse to stellar dimensions. This problem can be solved by various physical effects, such as:

1. Fragmentation of the core into a binary or multiple system
2. Collapse of the cloud into a central stellar object surrounded by an orbiting disk, which contains most of the angular momentum.

¹Credit: ESO/Igor Chekalin <https://www.eso.org/public/images/eso1105a/>

²Credit: ESO <https://www.eso.org/public/images/eso1233a/>

2.1.2 Star formation phases

The temperature in the ISM vary greatly and in the colder areas (~ 10 K) hydrogen (with some traces of other elements) exists in molecular form in giant molecular clouds. These objects are very inhomogenous, with the densest regions as much as a 1000 times the density of the more rarefied regions (Figure 2.2a [6]). Inside molecular clouds, the gas pressures are higher than those in the surrounding interstellar medium, and almost all molecular clouds in our galaxy exhibit star formation [3].

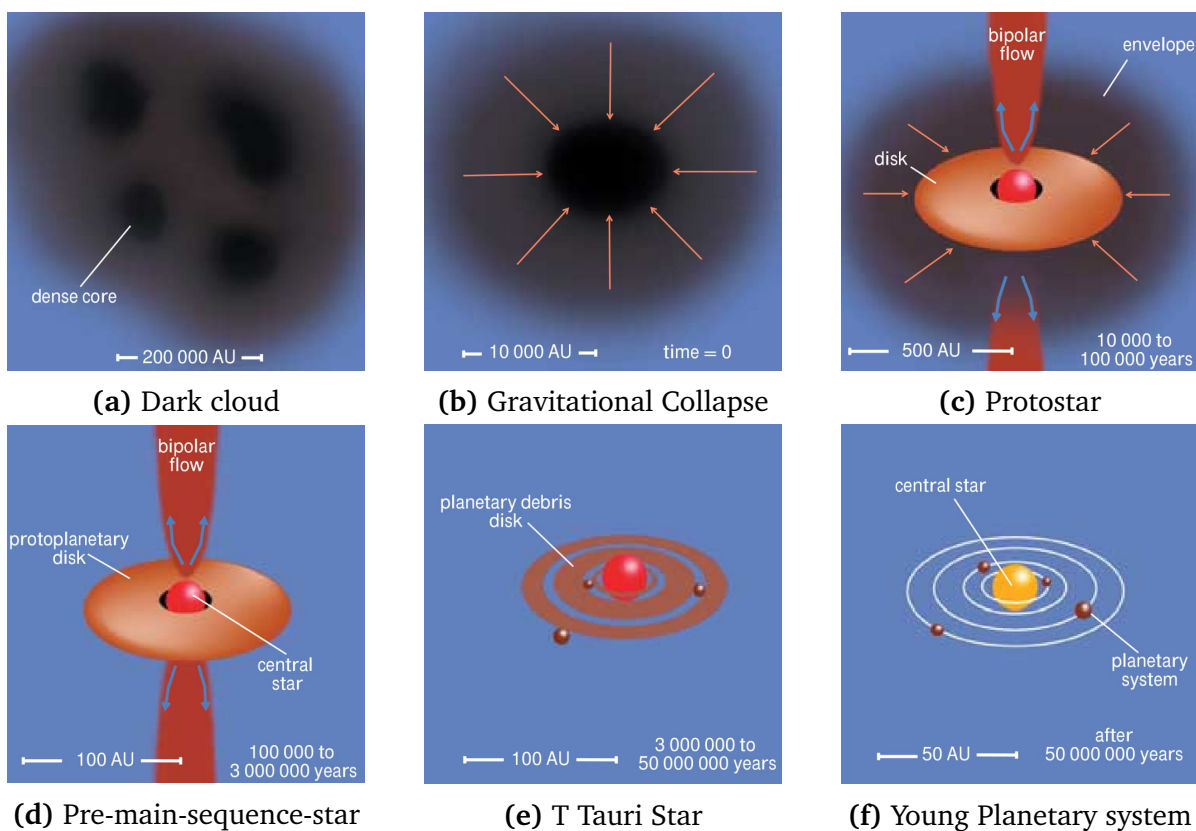


Figure 2.2: The stages of formation of a Sun-like star.

Molecular clouds are usually supported against their weight by thermal pressure, turbulent gas motion and magnetic fields within. By various mechanisms the clouds become unstable and begin to collapse under their own weight (Figure 2.2b). This could be due to long time scale evolution of the cloud or a turbulence, such as supersonic turbulances, random shock interactions in the ISM, supernova shocks, stellar winds and so on [3]. At the centre of the collapsing cloud a protostar forms (Figure 2.2c). The protostar continues to rapidly accumulate mass from the surrounding envelope of gas and dust over the course of about 100 000 years. During its lifetime the

protostar progressively increases in density and shrinks in size, accreting the infalling material and shedding mass through bipolar jets. The infalling material, which had been rotating relatively slowly, speeds up as it approaches the protostar due to conservation of angular momentum. Most matter from the envelope disperses or eventually flows onto the protostar, but some of it falls into orbits of various sizes depending on its velocity, forming a circumstellar disk. As the accretion process stops, the central globe of gas is no longer considered a protostar: it is now a pre-main-sequence (or PMS) star (Figure 2.2d). Protostars and PMS stars are grouped under the term young stellar objects (or YSO). The pre-main-sequence phase of evolution lasts for tens of millions of years and in its earliest phases, these objects are called T Tauri stars (derived from the archetypical star in the constellation Taurus). With no dusty envelopes, T Tauri stars are the youngest objects that can be observed with an optical telescope. They are surrounded by disks of dust and gas – often called protoplanetary disk and can continue to eject material in their bipolar jets (Figure 2.2e). After a few million years, much of the dust and gas in the protoplanetary disk dissipates, leaving a bare PMS star in the centre, sometimes orbited by a few large bodies in a remnant debris disk. In tens of millions of years, the force of gravity eventually triumphs over the outward thermal pressure of the gas within the star and the temperature of the star's interior raises to about 10 million Kelvins – hot enough to fuse Helium. This marks the arrival of the star on the main-sequence phase of its evolution (Figure 2.2f). This period is extremely stable, and may last for billions of years. The Sun is an example of a main-sequence star, which has been fusing hydrogen into Helium for 5 billions years, and is predicted to do so for 5 billion more.

2.2 Radiation

Before the properties of pre-main sequence stars and the surrounding circumstellar disks can be explored further, it is important to lay down the basics of radiative transfer and the underlying radiation mechanisms.

2.2.1 Absorption, emission and scattering

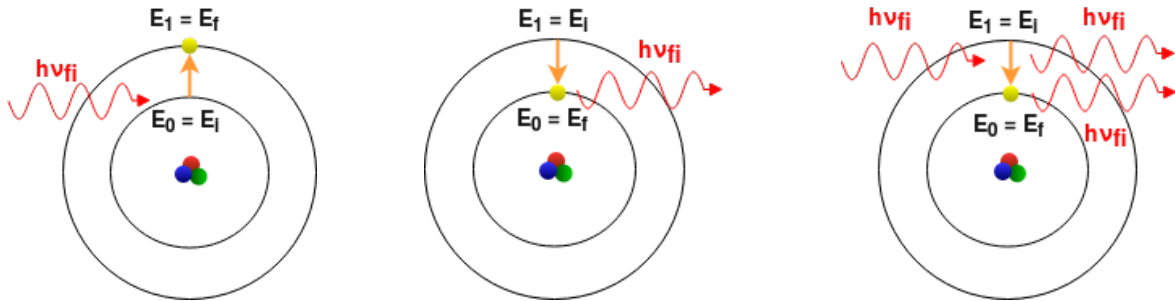
At atomic level, if the total energy decreases by ΔE the atom emits a quantum of electromagnetic radiation called a *photon*, whose frequency ν is determined by the equation [7]:

$$\Delta E = h\nu, \quad (2.1)$$

where $h = 6.6256 \cdot 10^{-34} \text{ Js}$ is the *Planck constant*. Consequently, if the same atom absorbs a photon of frequency ν , it gains energy ΔE .

The energy levels of an electron in an atom are quantized, limitting the frequencies at which an atom can absorb or emit radiation, corresponding to the difference between the initial state i and final state f of the system: $|E_f - E_i| = h\nu_{fi}$. A transition from a lower energetic state to a higher energetic state by assimilation of a photon of frequency $h\nu_{fi}$ is called **excitation** or **absorption** (Figure 2.3a). A typical lifetime for an excited state is 10^{-8} s , after which the atom may return to its lower state, radiating a photon, through the process of **spontaneous emission** (Figure 2.3b). Transitions to lower states (downward) can also be induced by another photon, whose frequency $\nu_{\text{photon}} = \nu_{fi}$ corresponds to the downward transition, interacting and perturbing the excited state. This process called **stimulated emission** (Figure 2.3c). While spontaneously emitted photons have randomly distributed phases and directions when leaving the atom, producing an incoherent radiation, the radiation produced through stimulated emission is coherent and propagates in the same direction as the induced radiation. **Scattering** is defined as a change in the direction of motion of a particle due to the interaction with the medium (collision with other particle). When referring to electromagnetic radiation, this process can be modeled as absorption of a photon, immediately followed by an instantaneous emission of the photon at the same wavelength, but in a different direction. On the macroscopic scale, the medium seems to reflect the radiation (e.g. atmospheric particles scatter blue light from the Sun).

Through absorption, spontaneous emission and stimulated emission the system's energetic states can change (Figure 2.3), this gives rise to an element-specific line spectrum (see 2.3d for Hydrogen). A hot gas under low pressures produces an emission spectrum of discrete lines. The same gas at a cooler temperature observed against a source of white light (continuous spectrum) shows dark absorption lines at the cor-



(a) **Absorption** occurs when a photon of frequency ν_{fi} is absorbed and the system, initially in a low energy state, is excited to a higher energy state.

(b) **Spontaneous emission** is the opposite process to absorption, in the sense that the system emits a photon with the energy corresponding to $\Delta E = h\nu_{fi} = h\nu_{if}$ as the system goes from the excited state to a lower energy state finally.

(c) **Stimulated emission** is the process in which emission occurs after a photon with exactly the same frequency as the emitted photon $h\nu_{fi}$ interacts with the excited state.



(d) **Hydrogen Spectra:** absorption (top) lines can be seen as dark (missing) lines against the continuous spectra of light & emission (bottom) lines in color ar at the same frequency as the corresponding absorption between the same states.

Figure 2.3: Spectral lines origin

responding frequencies for the same transitions as the emission lines[7]. In reality, the spectral lines are not infinitely narrow and sharp, but are somewhat broadened, having a shape called a line profile. There are various factors which contribute to line broadening, an intrinsic one being Heisenberg's *uncertainty principle* ($\Delta E \Delta t \approx \hbar$). AS a consequence, if a state has a lifetime τ_k , its corresponding energy can only physically be determined with an accuracy of $\Delta E_k = \hbar/\tau_k$. The uncertainty in the energy levels (And therefore in the wavelength) involved in a transition depends on the lifetimes of both the final and initial states, giving a **natural line width** γ (2.2). If only this effect is taken into consideration, the width γ is equal to the full width at half maximum

(FWHM), as this is the width of the line profile at a depth where the intensity is half of the maximum.

$$\gamma = \frac{1}{\tau_i} + \frac{1}{\tau_f} \quad (2.2)$$

The higher the temperature of a gas, the faster atoms move, causing the spectral lines to move due to the *Doppler effect*, thus, the shape of the line depends on the velocity distribution of individual atoms. The line profile due to Doppler shifts is called a Voigt profile, and is less sharp than the natural line profile, having a greater full width at half maximum. Other effects include pressure broadening and non-local broadening.

2.2.2 Blackbody radiation

A **blackbody** is a physically ideal object, which does not reflect or scatter radiation, but absorbs and re-emits radiation completely. Black holes are near-perfect black bodies, as they absorb all the incident radiation, and although planets and stars are not perfect blackbodies, black-body radiation is a good first approximation for the thermal energy they emit. The wavelength distribution of the radiation follows *Planck's Law* and depends only on the temperature T of the blackbody. The intensity B of the radiation at frequency ν is given by:

$$B_\nu(T) = \frac{2h\nu^3}{c^2} \frac{1}{e^{h\nu/kT} - 1}, \quad (2.3)$$

where h is *Planck's constant*, c is the *speed of light* ($3 \cdot 10^8 \text{ ms}^{-1}$), and k is the *Boltzmann constant* ($1.38 \cdot 10^{-23} \text{ JK}^{-1}$), giving the intensity B_ν the dimension $\text{W m}^{-2} \text{ Hz}^{-1} \text{ sterad}^{-1}$. The distribution can also be written as a function of wavelength:

$$B_\lambda(T) = \frac{2hc^2}{\lambda^5} \frac{1}{e^{hc/\lambda kT} - 1}, \quad (2.4)$$

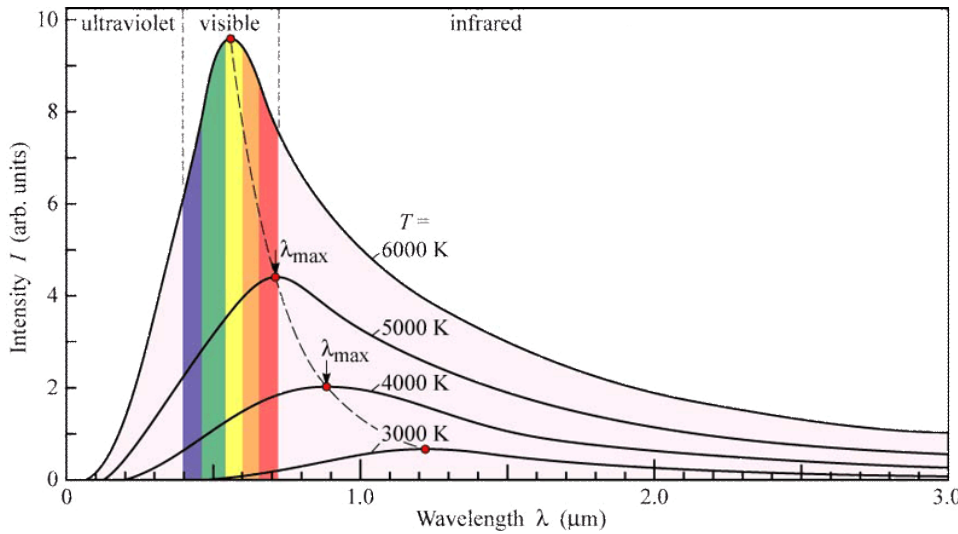


Figure 2.4: Intensity distribution of black bodies at different temperatures according to Planck's Law. The Sun, with a temperature of 5780K peaks in the area fo the spectrum corresponding to visible light. [?]

The total intensity can be calculated by integrating over the spectrum:

$$B(T) = \int_0^\infty B_\lambda(T) d\lambda = \int_0^\infty B_\nu(T) d\nu \quad (2.5)$$

By replacing (2.3) into (2.5) and taking out the independet variables the following is obtained:

$$B(T) = \frac{2h}{c^2} \int_0^\infty \frac{\nu^3}{e^{h\nu/kT} - 1} d\nu \quad (2.6)$$

Integrating by substitution of the integration variable with $x = h\nu/(kT)$, $d\nu = kT dx/h$ in (2.6) the following is obtained:

$$B(T) = \frac{2h}{c^2} \frac{k^4}{h^4} T^4 \int_0^\infty \frac{x^3}{e^x - 1} dx = \frac{2k^4 \pi^4}{c^2 h^3} \frac{T^4}{15} \quad (2.7)$$

The integral in (2.7) is not easy to evaluate, but it can easily be seen that it is constant in value (independent of temperature). The flux density F for isotropic radiation of intensity B is $F = \pi B$ so the flux can be written as:

$$F = \sigma T^4. \quad (2.8)$$

Equation (2.20) is the *Stefan-Boltzmann Law*, with $\sigma = 5.67 \cdot 10^{-8} \text{ W m}^{-2} \text{ K}^{-4}$, the *Stefan-Boltzmann constant*.

2.2.3 Radiative Transfer

The mechanism through which energy is transferred through the propagation of radiation through a medium is called radiative transfer. The propagation of radiation through a medium is governed by the aforementioned phenomena of absorption, emission, and scattering, where absorption leads to a gain in energy, emission leads to a loss of energy and scattering represents the redistribution of energy. The equation of radiative transfer can be easily derived.

Assume a source, such as a star, which is radiating like a blackbody at temperature T , and a small area of space, in a form of a cylinder of area dA , and radius dr , at a distance d from the source, such that it spans the solid angle $d\omega$: Figure 2.5.

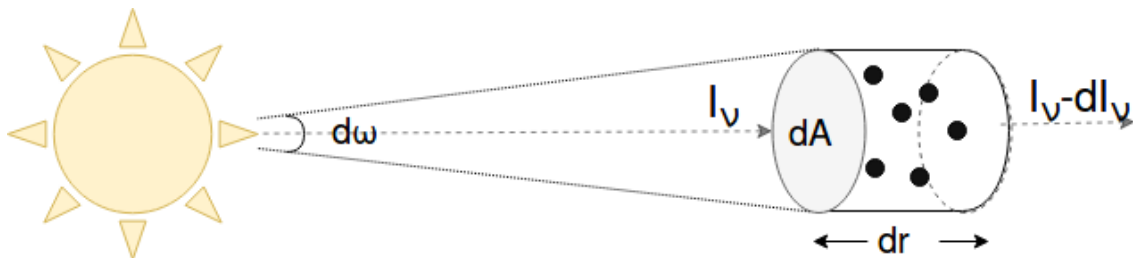


Figure 2.5

If the intensity changes by an amount dI_ν going through the cylinder, than in the time interval dt , the energy changes by:

$$dE = dI_\nu dA d\nu d\omega dt \quad (2.9)$$

This energy difference must be equal to the absorption minus the emission in the cylinder element. The fraction of absorbed energy depends on the opacity of the medium at the given frequency ν :

$$dE_{\text{abs}} = \alpha_\nu I_\nu dr dA d\nu d\omega dt \quad (2.10)$$

Let the emission coefficient of the medium be j_ν , describing the amount of energy emitted at frequency ν , per Hertz, per unit time, into unit solid angle from unit volume, then the energy emitted is:

$$dE_{\text{em}} = j_\nu dr dA d\nu d\omega dt \quad (2.11)$$

By replacing (2.9), (2.10), (2.11) into the equation for conservation of energy

$$dE = -dE_{\text{abs}} + dE_{\text{em}}, \quad (2.12)$$

one obtains:

$$dI_\nu = -\alpha_\nu I_\nu dr + j_\nu dr \quad (2.13)$$

or

$$\frac{dI_\nu}{\alpha_\nu dr} = -I_\nu + \frac{j_\nu}{\alpha_\nu} \quad (2.14)$$

The **optical depth**, τ , in astrophysics is a measure of the extinction coefficient or absorptivity of a medium at a certain frequency ν . Therefore the total optical depth, expressing how much of the light will be absorbed by the medium through a certain path is the integral sum of the extinction coefficient α_ν along that path:

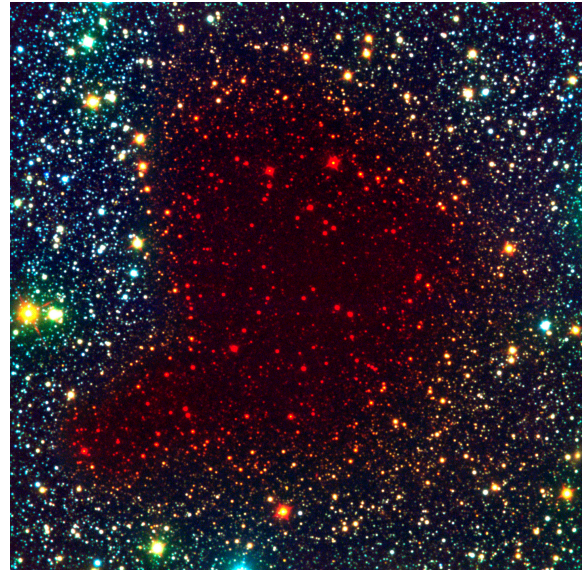
$$\tau_\nu = \int_0^r \alpha_\nu dr = \sigma N \quad (2.15)$$

, and it can also be expressed in terms of the number density N and the cross section σ . From the definition one can understand that an optically thick material, with a high value for the optical depth τ , is highly obscuring and does not let much of the light pass through. Figure 2.15 exemplifies this with a real celestial object.

The *source function* S_ν is a measure of the emission to absorbtion coefficient in the case of no scattering, indicateing how many photons are removed and replaced by new ones as a beam of light passes through the material:



(a) Barnard 68 three-color composite reproduced from one blue (B), one green-yellow (V) and one near-infrared (I) exposure¹



(b) Barnard 68, false-colour composite based on a visible (here rendered as blue), a near-infrared (green) and an infrared (red) image²

Figure 2.6: Comparing the two composite expositions of the same astronomical object, it can be clearly seen in 2.6a that the globule is optically thick for the visible spectrum, not letting any light from the stars behind pass through, while in 2.6b a multitude of stars appear in the infrared, colored red in the image, making the globule optically thin in the infrared region of the spectrum.

$$S_\nu = \frac{j_\nu}{\alpha_\nu} \quad (2.16)$$

By replacing the newly defined optical depth (2.15) and source function (2.16) into the derived equation (2.14) from the conservation of energy, the following is obtianed:

$$\frac{dI_\nu}{d\tau_\nu} = -I_\nu + S_\nu \quad (2.17)$$

¹Credit: ESO, <https://www.eso.org/public/images/eso0102a/>

²Credit: ESO, <https://www.eso.org/public/images/eso0102b/>

Equation (2.17) is the basic equation of radiative transfer. If the incident intensity $I_\nu < S_\nu$ is smaller than the source function, the intensity increases in the direction of propagation, meaning also the medium is emitting more than it is absorbing for the given frequency ν . Whereas, if the incident intensity is larger than the source function $I_\nu > S_\nu$, then $dI_\nu/d\tau < 0$ and the outgoing intensity will be smaller, meaning the medium is absorbant or optically thick at the given frequency. In equilibrium, the emitted and absorbed energies are equal, $I_\nu = S_\nu$, and the radiation of the medium is that of a blackbody, with the source function given by:

$$S_\nu = B_\nu(T) = \frac{2h\nu^3}{c^2} \frac{1}{\exp h\nu/kT - 1} \quad (2.18)$$

A formal solution to the radiative transfer equation (2.17) for the outgoing intensity is made up of an exponentially decay of the initial intensity (denoted $I_\nu(0)$) with the absorption coefficient plus the emission of the medium at the given frequency:

$$I_\nu(\tau_\nu) = I_\nu(0) \exp -\tau_\nu + \int_0^{\tau_\nu} \exp -(\tau_\nu - t) S_\nu(t) dt \quad (2.19)$$

The solution is only formal as S_ν is usually unknown must be solved for simultaneously with the intensity.

2.3 Stellar properties

2.3.1 Effective Temperature T_e [K]

Temperatures in the Universe range from 0K to millions of degrees, and the measure of the temperature depends on the physical phenomena underlying the definition of temperature. The most useful way to obtain a temperature is by fitting it against a blackbody spectra. The *effective temperature* T_e refers to the surface of the star and is defined as the temperature of a blackbody which radiates with the same total flux density as the star. In other words, for a value of the T_e which ensures the Stefan-Boltzmann law gives the correct flux density F on the surface of the star, we have

found the effective temperature. From (2.20), the flux density at the surface becomes then

$$F = \sigma T_e^4. \quad (2.20)$$

2.3.2 Luminosity $L_\star[\text{L}_\odot]$

The luminosity of a star is given by the total energy radiated per second from its surface. It can be calculated for a specific wavelength, or for all wavelengths (**Bolometric luminosity**). The brightness of the star as measured from Earth is called **Apparent Magnitude**¹ and it does not accurately describe the star's luminosity, as it is also dependent on the distance from the Earth to the star. Given that at a distance r from the source (star), the same amount of energy is spread to a sphere of surface area $4\pi r^2$, the flux density F falls off proportionally to $1/r^2$, as represented in Figure 2.7. Assuming an isotropically radiating star of luminosity L , the flux F at a distance r from the star would be given by the relation [7]:

$$L = 4\pi r^2 F \quad (2.21)$$

By replacing F from (2.20) in equation (2.21) we obtain the relationship between the radius, temperature and luminosity of a star.

$$L = 4\pi\sigma R^2 T_e^4 \quad (2.22)$$

¹The **Absolute Magnitude** of a star is defined as the apparent magnitude at exactly 10 parsec from the star.

²By Borb, CC BY-SA 3.0, <https://commons.wikimedia.org/w/index.php?curid=3816716>

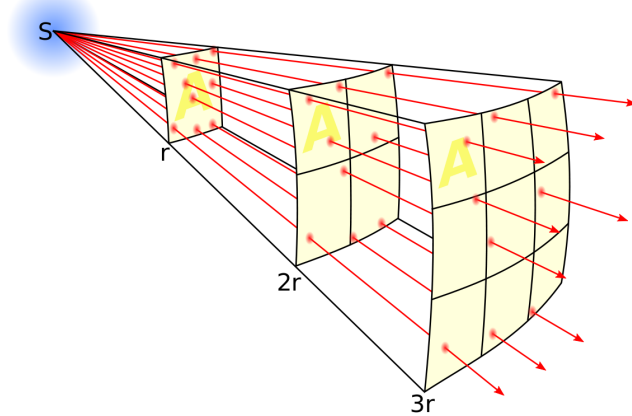


Figure 2.7: Inverse square law ¹: As the radius increases from r to $2r$, the same radiation passes now through 4 times the surface area A , and as the radius increase to $3r$, the surface area increases to $9A$.

2.3.3 Stellar Mass $M_\star[\text{M}_\odot]$

Stars are massive gaseous bodies which generate energy through nuclear fusion in the core, and release it as radiation. The mass of the star M_\star (usually expressed in terms of the mass of the Sun M_\odot) determines the star's properties (such as temperature, luminosity and size), but most importantly its evolution track. The pressure of the energy emitted from the core would cause the star to explode, were it not counteracted by the gravity of the surrounding material. When the sum of the gravitational and pressure force acting on a volume element is zero (Figure 2.8), hydrostatic equilibrium is reached, and the star is stable.

When the balance changes, however, so does the state of the star. Stars can have masses in a relatively small interval: if the mass of a star is less than 0.08 M_\odot or bigger than 100 M_\odot the star becomes unstable [9]. The smallest stellar masses observed are about 0.05 M_\odot , and the largest one could be up to 150 M_\odot [7]. These values are however approximate as they are based on an empirical mass–luminosity relation, which can be used to estimate stellar masses:

$$L \propto M^{3.8} \quad (2.23)$$

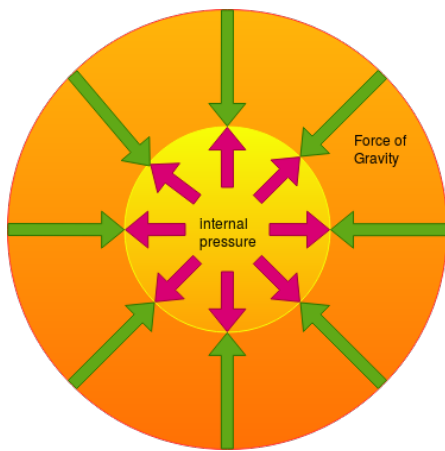


Figure 2.8: Hydrostatic equilibrium in stellar interiors is achieved when the **gravitational force** matches the **internal pressure** at each point.

It is important to note that the relations is only approximate, and can be considered valid for main-sequence stars. The only stars with accurately known masses are the ones found in binary systems, where the masses of the individual components can be determined by observing the motions of both components relative to the centre of mass. Less than half of all stars are single stars like the Sun, while more than 50 % belong to system consisting of two or more members (which is binary at some level).

2.3.4 Spectra

Most of the important information about the physical properties of stars come from studies of their spectra [7]. By means of dispersing the incoming light from stars we can observe their spectra and compare it to the spectra of known elements (e.g. the spectra of Hydrogen in Figure 2.3d, see appendix A).

The spectral classification scheme used at present is called the Harvard classification, as it was developed at the Harvard Observatory at the beginning of the 20th century by Annie Jump Cannon, and published in the Henry Draper Catalogue. The classification is based on lines that are mainly sensitive to the stellar temperature, such as the hydrogen Balmer lines, the lines of neutral helium, the iron lines and others mentioned in Table 2.1.

The spectral types were denoted alphabetically with a capital letter, subsequently, in order of decreasing temperature the classification became

C
 O–B–A–F–G–K–M–L–T
 S

with some additional notations (Q for novae, P for planetary nebulae and W for Wolf–Rayet stars). The spectral classes C and S represent parallel branches to types G–M, differing in their surface chemical composition. The most recent addition are the spectral classes L and T continuing the sequence beyond M, representing brown dwarfs. The spectral classes are divided into subclasses denoted by the numbers $\overline{0..9}$, with decimal sometimes being used.

| Type | Proeminent Spectral Lines | Color | Temperature |
|------|---|--------------|--|
| O | He^+ , He, H, O^{2+} , N^{2+} , C^{2+} , Si^{2+} | Blue |  $\sim 30\,000\text{ K}$ |
| B | He, H, C^+ , O^+ , N^+ , Fe^{2+} , Mg^{2+} | Blue-white |  $15\,000\text{ K}$ |
| A | He, ionized metals | White |  $9\,000\text{ K}$ |
| F | H, Ca^+ , Ti^+ , Fe^+ | Yellow-white |  $7\,000\text{ K}$ |
| G | Ca^+ , Fe, Ti, Mg, H, some molecular bands | Yellow |  $5\,500\text{ K}$ |
| K | Ca^+ , H, molecular bands | Orange |  $4\,000\text{ K}$ |
| M | TiO, Ca, molecular bands | Red |  $\sim 3\,000\text{ K}$ |

Table 2.1: Spectral stellar types

An alternative to the Harvard classification, which only takes into account the effect of temperature on the spectrum, is the Yerkes or MKK classification, which takes into account the luminosity of the stars (even for the same effective temperature), determined from spectral lines that depend strongly on the stellar surface gravity, which is closely related to the luminosity. Six different luminosity classes are distinguished, denoted by Roman numerals (the Sun is G2 V):

- Ia most luminous supergiants
- Ib less luminous supergiants
- II luminous giants
- III normal giants
- IV subgiants
- V main sequence stars (dwarfs)

2.3.5 HR Diagram

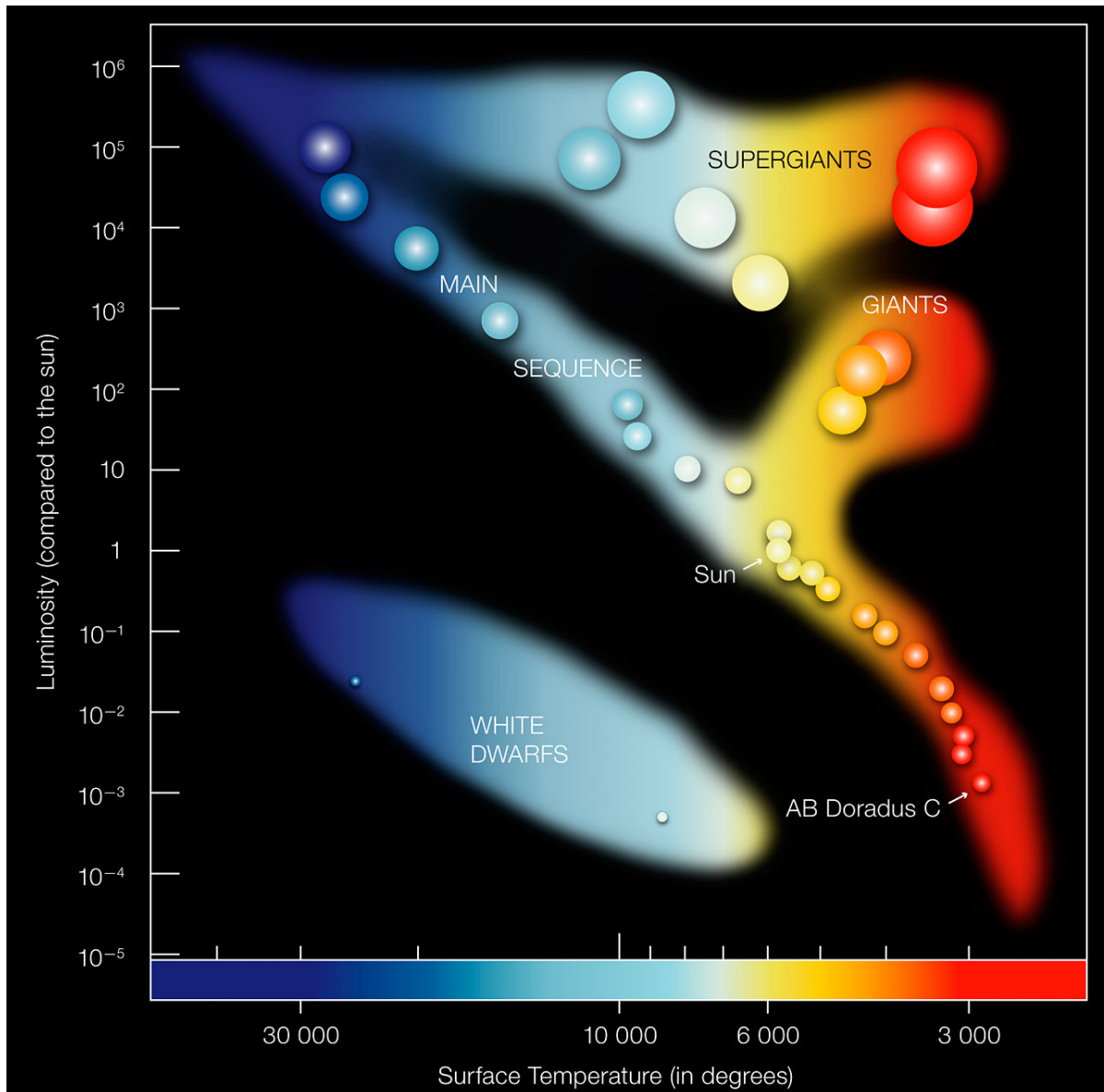


Figure 2.9: Herzsprung-Russell Diagram: In the Hertzprung-Russell diagram the temperatures of stars are plotted against their luminosities. The position of a star in the diagram provides information about its present stage and its mass. Stars that burn hydrogen into helium lie on the diagonal main sequence. The Sun is situated about the middle of the main sequence. **Credit:**ESO

The relation between the stellar properties of luminosity, effective temperature (or spectral type) and radius were studied by the physicists Ejnar Herzsprung and Henry Russell at the beginning of the 20th century. Their studies produced a very important aid in studies of stellar evolution, the Hertzsprung-Russell Diagram, or simply HR

diagram (Figure 2.9). One might have expected a uniform distribution of temperatures and luminosities, but it is found that most stars lie on the Main Sequence – the diagonal going from upper left to lower right. On the other diagonal, from lower left to upper right, the radii of the star increase (in accordance to equation 2.22). It is notable as well that the yellow and red stars (spectral types G–K–M) appear to be clustered into either the dwarf stars of the main sequence or the giants. The supergiants have an almost horizontal sequence, while the red giant branch rises from the main sequence around the temperature mark of the Sun. Below the main sequence, there is the group of white dwarfs, which are quite faint and difficult to observe.

Protostars enter the main sequence as their radius decreases and their temperature increases. In the main sequence stars are most stable, but they will eventually exhaust all the hydrogen. When this happens, the star leaves the main sequence and, depending on their mass, they have various destinies. Low mass stars ($\sim 0.5M_{\odot}$) will not have sufficient gravity to heat the core to high enough temperatures and pressures for fusing helium. They will cool down and become Red Dwarfs, like *AB Doradus C* in Figure 2.9. *AB Dor C* has a temperature of about 3000K and a luminosity which is 0.2% that of the Sun and it will never leave the main sequence. Stars similar to the Sun will expand and shed their exterior layers, as they run out of hydrogen, they will then collapse again before burning their Helium reserves and become a Red Giant before collapsing again into a White Dwarf. Bigger stars will expand to Super Giants, fusing more heavy elements. They will end their lives most spectacularly with a supernova, which will leave behind a neutron star for a star with more than $1.4M_{\odot}$ or a black hole for stars with a mass of more than $3M_{\odot}$ [9].

2.3.6 Variable Stars

Stars with changing brightness (or absolute magnitudes) are called *variables* or *variable stars* (about 40,000 stars known or suspected to be variable [7]). Technically, all stars are variable, given that their structure and brightness change as they evolve. Although the changes are usually slow, some evolutionary phases can be extremely rapid, or may present periodic variations, for example pulsations of the outer layers of a star. Small variations in stellar brightness are also caused by dark or light spots on a star's surface, as it rotates about its axis. The magnitude variation as a function of time is called the lightcurve of a star (Figure 2.10). From this the amplitude and period of the variation can be determined, if periodic.

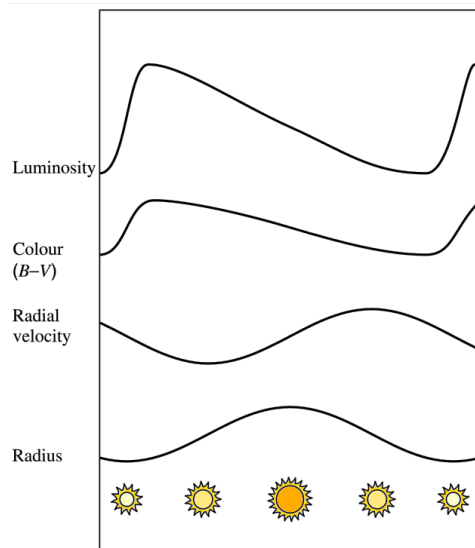


Figure 2.10: Variation of brightness, color and size of a cepheid¹ during its pulsation. The uppermost curve, describing luminosity is called the lightcurve. **Credit:** Adapted from [7]

Variables are classified based on the shape of their lightcurve, the spectral class and the observed motions in mainly three categories: pulsating, eruptive and eclipsing variables. A pulsating variable is an intrinsic variable, whose exterior layers are dilating and contracting, trying to reach an equilibrium between the gravitational force pushing inwards and the gas pressure pushing outwards. In the case of many pulsating variables (including cepheids³) the period of variation of the star is proportional to its luminosity. The diameter may double during the pulsation, but usually the main cause of light variation is the periodic variation of surface temperature. As seen in equation (2.22) $L \propto T_e^4$ and a small change in effective temperature leads to a large brightness variation. Stars with surface temperatures of 6000–9000 K are liable to this instability and the corresponding section of the HR diagram is called the cepheid instability strip. There are various pulsating variable stars with periods up to 500 days.

The eruptive variables exhibit instead of a regular pulsation a sudden outburst in which material is ejected into space. These stars are usually surrounded by a gas shell or interstellar matter. Flare stars are young stars which present flare outbursts on the surface at irregular intervals. Such a flare can cause a brightening by up to 4-5

³Among the most important pulsating variables are the **cepheids**, named after δ Cephei. They are supergiants of spectral class F–K, with periods of 1–50 days and amplitudes of 0.1–2.5 magnitudes in their variability

magnitudes [7]. Although this process is still not fully understood, it is common that a protostar and its accretion disc to cause jet-like flares as seen in Figure 2.13b.



Figure 2.11: Image of Herbig-Haro object (HH) 212, located in a dense star-forming region of the Horsehead Nebula with very large almost symmetric flares in orange. The central star is very young (thousands of years old) and it can be observed masked by the surrounding dusty disk (central dark region from which flares seem to originate), which is seen here edge-on. The star's pulses vary quite regularly, and over a short timescale (maybe even as short as 30 years). Further out from the centre, large bow shocks caused by ejected gas colliding with dust and gas at speeds of several hundred kilometres per second spread out into interstellar space. **Credit:** ESO/M. McCaughrean <https://www.eso.org/public/images/potw1541a/>

A flare lights up in a few seconds, and fades away in a few minutes, but the same star can flare up several times in one day. Novae and supernovae are also included in this category, but the T Tauri are the most interesting flare stars, and are one of the topics of concern of the present thesis. These stars are newly formed and just contracting toward the main-sequence. Such stars, in the process of formation, may change brightness very rapidly and commonly have irregular brightness variations (*FU Orionis* brightened in 1937 by 6 magnitudes). In 1969 *V1057 Cygni* brightned by six magnitues, and had remained fairly constant since.

The third category is the eclipsing variables. As the name suggests, these are usually binary systems in which the components periodically pass in front of each other. The variability is not related to any physical change in the star, and is apparent. In addition, a few rotating variables with an uneven distribution of temperature on the surface are known. They have periods of about 1 to 25 days and the changes are small, less than 0.1 magnitudes.

2.3.7 T Tauri stars

T Tauri stars were briefly mentioned in the previous section 2.3.6. It is important to define them, as they are the type of stars of interest to this thesis, and the relevant basis has been explored in order to fully understand their definition. They are a type of young pre-main-sequence variable stars in the process of contracting towards the main sequence. T Tauri stars usually have masses lower than 2 solar masses, and are of spectral types F, G, K or M. Their surface temperatures are similar to those of main-sequence stars of the same mass, but they are significantly more luminous because their radii are larger. Similar young pre-main-sequence stars, are Herbig Ae/Be type stars. They have masses between 2 and $8 M_{\odot}$ and are of spectral type A or B. They may sometimes show significant brightness variability. As they are not in the main sequence yet, both stellar types are not burning hydrogen, and are powered by gravitational energy released as the stars contract.

2.4 Circumstellar Disks

As seen in section 2.1, as clouds collapse into protostars, much of the angular momentum of the collapsing cloud is taken up by a circumstellar disk of gas and dust, which lasts 1–10 Myr before being photodissipated. It is thought that angular momentum has been significantly reduced by magnetic coupling between the star and the disk and also through the outflow in the poles, which is strongest during the protostellar phase. A schematic of a typical circularly-symmetrical disk can be seen in Figure 2.12. Even though the disks usually contain only a few percent of the material going into a young star, they are of great interest to study, because they are the place where planets may form.

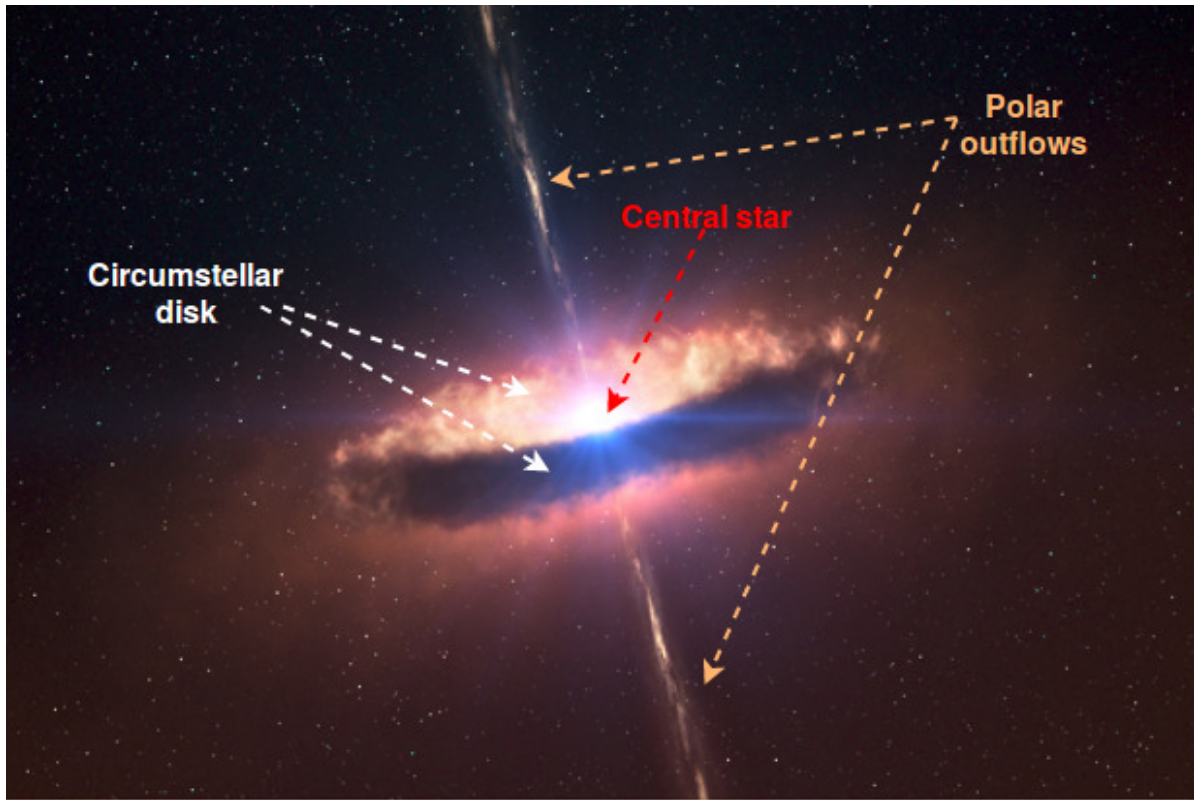
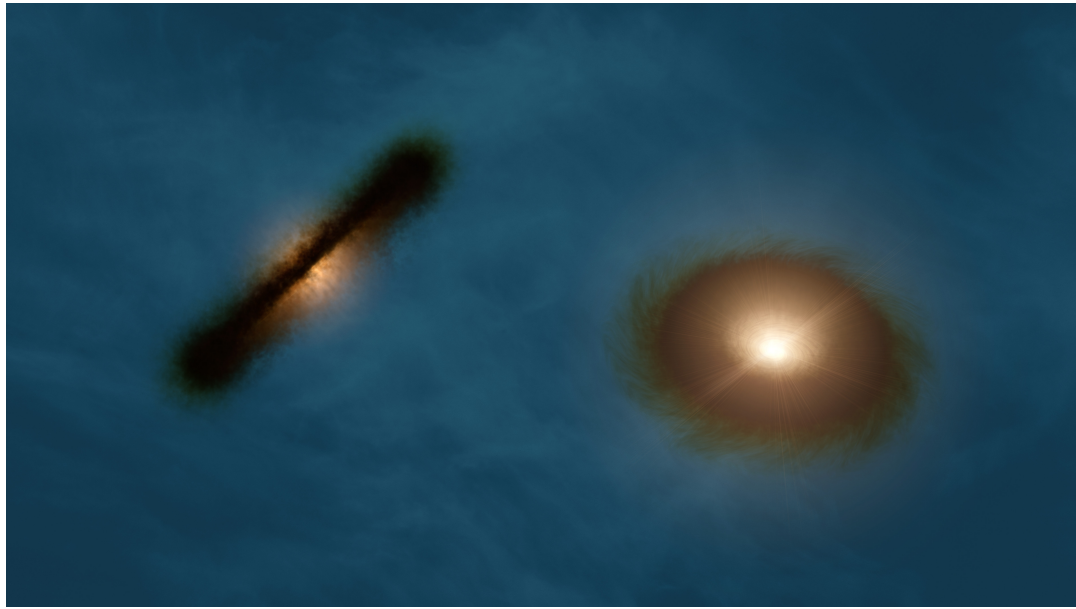
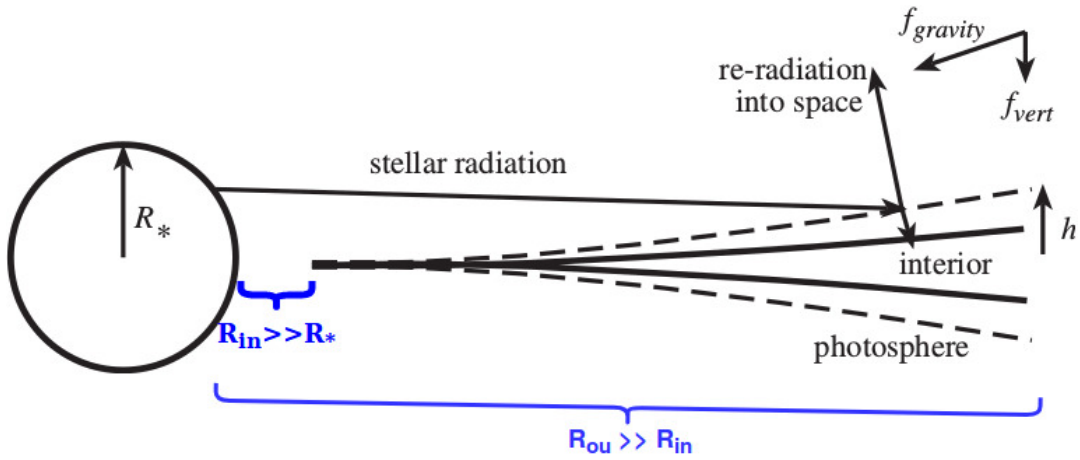


Figure 2.12: Artist impression (with added annotations) of pre-main-sequence star with disk. The disk extends to about 130 AU, and has a mass similar to the star. Jets can be observed at either pole of the star, spewing matter. **Credit:** ESO/L. Calçada/M. Kornmesser <https://www.eso.org/public/images/eso1029a/>

How common are circumstellar disks? Using data from the IRAS sky survey, two teams [4] and [1] discovered that approximately half of the T-Tauri stars observed have far infrared spectral energy distributions (SEDs), characteristic of heated dust and not of the photosphere. The relative low visual extinction (absorbed light from the star) suggested that the dust was in a flattened distribution. The first pictures of disks taken with the Hubble Space Telescope demonstrated clearly that the dust distribution followed the theoretical pattern of a disk [2]. Circumstellar disks (2.13a) are gently flared in the outer region due to the warming of the matter, and have some edge at a distance from the star (called further inner radius of the disk R_{in} in as in Figure 2.13b), and are heated mainly by radiation (as opposed to accretion). Most young disks are also accompanied by mass losses in columns around the polar axes.



(a) Artist impression of two circumstellar disks. The one on the left is seen edge on by the observer, while the disk on the right is almost face-on with a slight incline towards the observer.



(b) Schematic of star with section through flared circumstellar disk. The radius of the star R_* is usually a few solar radii R_\odot , while the rim of the disk approaches the star usually at a couple of astronomical units. Between the star and the inner radius of the disk R_{in} all dust is considered to have been accreted, due to unstable orbits, or the temperatures are too high for the dust to exist, making the dust density in this area nul. The disks outer radius is hard to distinguish as a low density, but non-zero distribution of dust may exist beyond the outer radius R_{out} , which is usually a couple of hundred astronomical units.

2.4.1 Interstellar Dust

Though originally thought as transparent, the interstellar medium is actually filled with dust, which also forms circumstellar disks. The dust was first observed when deducing that the apparent magnitude of stars is dimmed by some intervening material. Extinction due to dust varies with direction and is due to the particles having diameters near the wavelength of light ($0.01 - 0.2\mu m$). Such particles scatter light extremely efficiently. Gas can also cause extinction by scattering, but the efficiency per unit mass is much smaller.

Interstellar dust particles can cause extinction in two ways [7]

- Through absorption the radiant energy is transformed into heat, which is then re-radiated at infrared wavelengths corresponding to the temperature of the dust particles.
- Through scattering the direction of light propagation is changed, leading to a reduced intensity in the original direction of propagation.

For simplicity in calculating the coefficient of extinction C_{ext} for dust particles, they are assumed to be spheres with the same radius a , and therefore geometrical cross-section πa^2 .

$$C_{\text{ext}} = Q_{\text{ext}} \pi a^2, \quad (2.24)$$

where Q_{ext} is the extinction efficiency factor. Consider a volume element with cross section dA , incident to the radiation, and length dl . If the particle density is n , the total number of particles in a unit volume is $N = ndAdl$, while the fraction of the area covered by the particles will be C_{ext}/dA . On the basis of the previous equation (2.15), the optical depth over a path of length r can be expressed as a function of the extinction coefficient as:

$$\tau = N\sigma = \int_0^r nC_{\text{ext}}dl \approx C_{\text{ext}}\bar{n}r \approx Q_{\text{ext}}\pi a^2 \bar{n}r \quad (2.25)$$

where \bar{n} is the average density along the path.

The extinction factor $Q_{\text{ext}} = Q_{\text{abs}} + Q_{\text{sca}}$ is the sum of the absorption and the scattering extinction factors, and can be calculated for a given frequency from the quantity $x = 2\pi a/\lambda$, where a is the radius of the dust particles, and the refractive index m ($Q_{\text{ext}} = Q_{\text{ext}}(x, m)$). When $x \ll 1$, the particle is much smaller than the wavelength and elastic or Rayleigh scattering occurs, whereas for $x \geq 1$ Mie scattering occurs. An observable phenomena that occurs due to dust is the **reddening** of stars due to the fact that extinction becomes larger for shorter wavelengths. This means that going from red to ultraviolet the extinction is roughly inversely proportional to wavelength. For this reason, the light of distant stars is redder than would be expected on the basis of their spectral class. At the same time, if a dust cloud is close to a bright star, it will reflect much of the light, moreso in the blue end of the spectrum. Individual dust clouds can be observed as bright reflection nebulae.

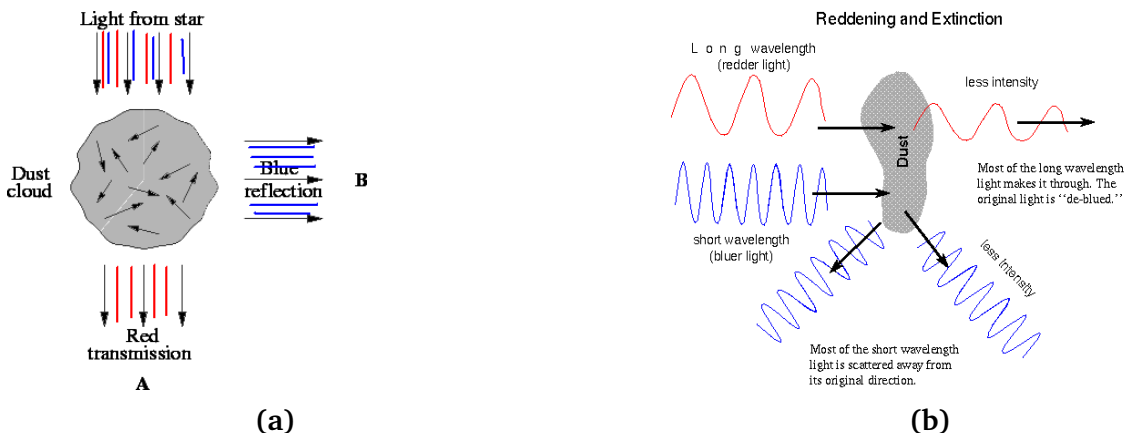


Figure 2.14: Dust extinction and scattering

Dust particles polarize light from the stars. Since this effect could not be produced by spherical particles, the interstellar dust particles must be non-spherical in shape. Through alignment by the interstellar magnetic field, dust particles will polarize radiation passing through a cloud. The degree of polarisation and its wavelength dependence rest on the properties of the dust particles. In addition to scattering radiation, dust also absorbs energy and re-radiate it at infrared wavelengths, corresponding to their temperature. For interstellar dust (including in dark nebulae) at 10 – 20K, the corresponding peak according to Plack's law would be at 300 – 150 μm , while for dust at the inner edge of a circumstellar disk, near a hot star, the temperatures may be 100 – 600K and the maximum emission is then at 30 – 5 μm , illustrated in Figure 2.15a. Dust can be detected and observed in the infrared due to its strong thermal emission.

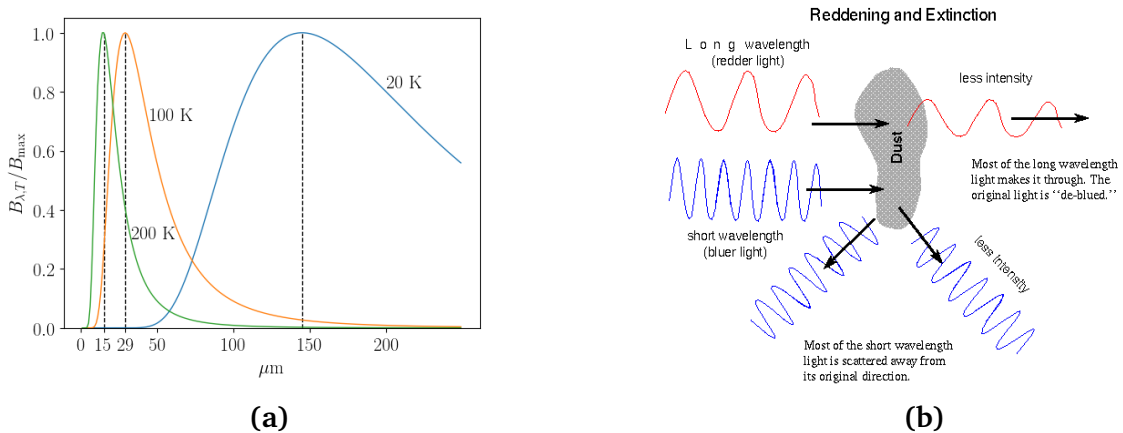


Figure 2.15: Dust extinction and scattering

From the peaks in the extinction curves, it may be concluded that interstellar dust contains water ice and silicates, as well as graphite. A typical composition [11] is 63.5% astrosilicate combined with carbon in different polarisations. The sizes of the grains, deduced from their scattering properties are usually smaller than $1\mu\text{m}$. Dust grains are assumed to be formed in the atmospheres of stars of late spectral types (K, M), as gas condenses into grains, which are then expelled into interstellar space by radiation pressure. Although the mass of interstellar gas is a hundred times larger than that of dust, gas is less easily observable as it does not in general cause great extinction of light.

Chapter 3

Method

3.1 T Tauri Data

| Star name | Type | distance d [pc] | T_{eff} [K] | L [L_{\odot}] | L_{min} [L_{\odot}] | L_{max} [L_{\odot}] |
|--------------|---------|-------------------|----------------------|---------------------|----------------------------------|----------------------------------|
| LkHalpha330 | T Tauri | 250 | 5800 | 11 | 7 | 16 |
| LkCa16 | T Tauri | 142 | 4350 | 0.8 | 0.6 | 1 |
| DRTau | T Tauri | 142 | 4060 | 1.1 | 0.9 | 1.3 |
| GMAur | T Tauri | 142 | 4730 | 1.2 | 0.8 | 1.6 |
| TCha | T Tauri | 108 | 5890 | 1.2 | 0.5 | 3.1 |
| HD142560 | T Tauri | 150 | 4000 | 3.7 | 2.2 | 5.6 |
| HD143006 | T Tauri | 145 | 5884 | 3.4 | 2.7 | 4.2 |
| V2246OPH | T Tauri | 120 | 5248 | 7.5 | 6.3 | 9.5 |
| HBC639 | T Tauri | 120 | 5250 | 8.1 | 4.8 | 11.8 |
| ELIAS2-24 | T Tauri | 120 | 4266 | 1.8 | 1.1 | 2 |
| ELIAS2-28 | T Tauri | 120 | 4169 | 0.3 | 0.2 | 0.6 |
| V2129OPH | T Tauri | 120 | 3981 | 1.3 | 0.8 | 1.7 |
| V2062OPH | T Tauri | 120 | 4900 | 1.5 | 1 | 2.1 |

$$L \propto \sigma T_{\text{eff}}^4 4\pi R^2 \quad (3.1)$$

$$\frac{L}{L_\odot} = \left(\frac{T}{T_\odot}\right)^4 \left(\frac{R}{R_\odot}\right)^2 \quad (3.2)$$

$$T_\odot \approx 5780\text{K} \quad (3.3)$$

| | |
|------------------|-------------------------|
| Spectral type | late K, F, G or early M |
| T_{eff} | 3500 – 9000 K |
| M_\star | 1 – 3 M_\odot |
| R_\star | 2 – 6 R_\odot |
| L_\star | 0.1 – 50 L_\odot |

$$T_\odot \approx 5780\text{K} \quad (3.4)$$

$$\Delta x = \mathbf{b} \cdot \mathbf{s} \quad (3.5)$$

$$V = 0 \implies \Delta x = b \cdot s \cdot \theta = (2k + 1)\lambda \implies b = \frac{(2k + 1)\lambda}{s\theta} \quad (3.6)$$

| | |
|-------------------|-----------------------------|
| M_{disk} | $10^{-5} - 10^{-7} M_\odot$ |
| R_{in} | 0.07 – 10 AU |
| R_{out} | 100 – 300 AU |

$$\rho(r, z)^{\text{Sh-Su}} = \left(\frac{r}{100}\right)^{-\alpha} \exp\left(-\frac{1}{2} \frac{z^2}{h(r)^2}\right),$$

$$h(r) = h_0 \left(\frac{r}{100}\right)^\beta, \quad \alpha = 2.625, \beta = 1.125, h_0 = 10 \text{AU}$$
(3.7)

$$\rho(r, z)^{\text{Ly-P}} = \rho(r, z)^{\text{Sh-Su}} \exp\left(\left(-\frac{r}{100}\right)^{(2+\beta-\alpha)}\right)$$

Figure 8: Dust number density in xz -plane, $L = 1.5L_\odot$, $T = 6000\text{K}$, $R_{\text{in}} = 1\text{AU}$ **Figure 9:** Temperature in xz -plane, $L = 1.5L_\odot$, $T = 6000\text{K}$, $R_{\text{in}} = 1\text{AU}$

(Credit: Kirchschlager, 2017)

| DR Tau Parameters | |
|-------------------|---------------------------|
| T_\star | 4050 K |
| L_\star | $0.9 - 15 L_\odot$ |
| T_{accr} | 8000 K |
| L_{accr} | $1 L_\odot$ |
| R_{in} | 0.065 AU |
| R_{ou} | 350 AU |
| β | 1.025 |
| h_0 | 10.0 AU |
| M_{disk} | $3 \cdot 10^{-3} M_\odot$ |

The Van-Cittert / Zernike theorem: the complex visibility μ , for a non-coherent and almost monochromatic extended source is the normalized Fourier Transform (\mathcal{FT}) of the brightness distribution ($I(x, y)$):

| Name | Number of Telescopes | Diameter [m] | Maximum baseline | λ |
|--------------|----------------------|--------------|------------------|-----------|
| Keck I | 2 | 10 | 85 | NIR, MIR |
| VLTI/MIDI | 2/2 | 8/1.8 | 130 / 200 | MIR |
| VLTI/PIONIER | 4 | 8/1.8 | 130 / 200 | NIR |
| VLTI/MATISSE | 4 | 8/1.8 | 200 | NIR, MIR |
| VLTI/AMBER | 3 | 8/1.8 | 140 | NIR |
| ALMA | 66 | 12 | 16 000 | radio |

$$\mu(\mathbf{b}, \lambda) = \frac{\mathcal{FT}(I(x, y))}{\iint I(x, y)} \quad (3.8)$$

$$\mu(u, v) = \frac{\iint_{-\infty}^{\infty} I(x, y) e^{2\pi i(ux+vy)} dx dy}{\iint_{-\infty}^{\infty} I(x, y) dx dy}, \text{ where } u = \frac{b_x}{\lambda}, v = \frac{b_y}{\lambda} \quad (3.9)$$

$$V(u, v) = \|\mu(u, v)\| \in [0, 1] \quad (3.10)$$

$$\lambda = 8\mu m \quad (3.11)$$

$$\mathcal{FT}(u, v) \quad (3.12)$$

Bibliography

- 1 A study of the stellar population in the LYNDS 1641 dark cloud. I - The IRAS catalog sources. In: *Astrophysical Journal Supplement Series* 71 (1989), S. 183–217
- 2 BECKWITH, S. V. W.: Circumstellar Disks. In: LADA, C. J. (Hrsg.) ; KYLAFIS, N. D. (Hrsg.): *NATO Advanced Science Institutes (ASI) Series C* Bd. 540, 1999 (NATO Advanced Science Institutes (ASI) Series C), S. 579
- 3 BODENHEIMER, P. H.: *Principles of Star Formation*. Springer, 2011. – ISBN 978-3-642-15062-3
- 4 COHEN, MARTIN AND EMERSON, J. P. AND BEICHMAN, C. A.: A reexamination of luminosity sources in T Tauri stars. I - Taurus-Auriga. In: *Astrophysical Journal* 339 (1989), S. 455–473
- 5 FIXSEN, D. J.: The Temperature of the Cosmic Microwave Background. In: *The Astrophysical Journal* 707 (2009), Nr. 2, 916. <http://stacks.iop.org/0004-637X/707/i=2/a=916>
- 6 GREENE, T. P.: Protostars. In: *American Scientist* 89 (2001), S. 316–325
- 7 KARTTUNEN, H. ; KRÖGER, P. ; OJA, H. ; POUTANEN, M. ; DONNER, K. J.: *Fundamental Astronomy*. 6. Springer, 2017. <http://dx.doi.org/https://doi.org/10.1007/978-3-662-53045-0>. – ISBN 978-3-662-53044-3
- 8 KIRCHSCHLAGER, F. ; WOLF, S. ; KRIVOV, A. V. ; MUTSCHKE, H. ; BRUNNGRÄBER, R. : Constraints on the structure of hot exozodiacal dust belts. In: 467 (2017), Mai, S. 1614–1626. <http://dx.doi.org/10.1093/mnras/stx202>. – DOI 10.1093/mnras/stx202

-
- 9 REESE, M. (Hrsg.): *Universe: The Definitive Visual Guide*. DK ADULT, 2005. – ISBN 0756613647
 - 10 SINGH, R. ; MANI, V. ; VISHWAKARMA, K. : Evaluating Age of Universe by Photometric Analysis of Globular Clusters. 42 (2018), Jul., S. E1.16–26–18
 - 11 WEINGARTNER, J. C. ; DRAINE, B. T.: Dust Grain-Size Distributions and Extinction in the Milky Way, Large Magellanic Cloud, and Small Magellanic Cloud. In: *The Astrophysical Journal* 548 (2001), S. 296–309

Selbstständigkeitserklärung

Ich versichere hiermit, dass ich die vorliegende Arbeit selbstständig verfasst und keine anderen als die angegebenen Quellen und Hilfsmittel benutzt habe.

Rostock, (Datum)